



**HAL**  
open science

## **Relation of the ischaemic substrate to left ventricular remodelling by cardiac magnetic resonance at 1.5 T in rabbits.**

Nicolas Mansencal, Renaud Tissier, Jean-François Deux, Bijan Ghaleh, Nicolas Couvreur, Mario Rienzo, Pascal Guéret, Alain Rahmouni, Alain Berdeaux, Jérôme Garot

### ► To cite this version:

Nicolas Mansencal, Renaud Tissier, Jean-François Deux, Bijan Ghaleh, Nicolas Couvreur, et al.. Relation of the ischaemic substrate to left ventricular remodelling by cardiac magnetic resonance at 1.5 T in rabbits.. *European Radiology*, 2010, 20 (5), pp.1214-20. 10.1007/s00330-009-1660-7. inserm-00476405

**HAL Id: inserm-00476405**

**<https://inserm.hal.science/inserm-00476405>**

Submitted on 26 Apr 2010

**HAL** is a multi-disciplinary open access archive for the deposit and dissemination of scientific research documents, whether they are published or not. The documents may come from teaching and research institutions in France or abroad, or from public or private research centers.

L'archive ouverte pluridisciplinaire **HAL**, est destinée au dépôt et à la diffusion de documents scientifiques de niveau recherche, publiés ou non, émanant des établissements d'enseignement et de recherche français ou étrangers, des laboratoires publics ou privés.

# Relation of the ischaemic substrate to left ventricular remodelling by cardiac magnetic resonance at 1.5T in rabbits

Nicolas Mansencal,<sup>1</sup> Renaud Tissier,<sup>1</sup> Jean-François Deux,<sup>2</sup> Bijan Ghaleh,<sup>1</sup> Nicolas Couvreur,<sup>1</sup> Mario Rienzo,<sup>2</sup> Pascal Guéret,<sup>3</sup> Alain Rahmouni,<sup>2</sup> Alain Berdeaux,<sup>1</sup> Jérôme Garot,<sup>1,3</sup>

From <sup>1</sup>INSERM U841, IMRB, Faculté de médecine, Université Paris 12 et Ecole Nationale Vétérinaire d'Alfort; Maison-Alfort, France <sup>2</sup>Department of Radiology and <sup>3</sup>Department of Cardiology, University Hospital Henri Mondor, Assistance Publique-Hôpitaux de Paris, Créteil, France.

**Short title:** Cardiac Magnetic Resonance at 1.5T in Rabbits

## Grant information:

Dr Mansencal was supported by a grant from the *Fédération Française de Cardiologie* Paris, France. Prof. Garot was supported in part by the “*Dotation à la Recherche par équipe*” of the *Maison du Cœur*, Paris, France.

None of the authors has any conflict of interest to declare.

## Correspondence:

Jérôme Garot, MD, PhD  
CMR Department  
Institut Hospitalier Jacques Cartier  
6 Avenue du Noyer Lambert  
91300 Massy  
France  
Tel: + 33 1 60 13 46 02  
Fax: +33 1 60 13 46 03  
Email: j.garot@icps.com.fr

**Abstract**

**Objectives:** Contrast-enhanced cardiac magnetic resonance (CMR) for infarct sizing has been validated in large animals, but studies and follow-up are restricted. We sought to 1) validate CMR for assessment of myocardial area at risk (MAR) and infarct size (IS) in a rabbit model of reperfused myocardial infarction (MI); 2) analyse the relation between ischaemic substrates and subsequent left ventricular (LV) remodelling.

**Methods:** Experimental reperfused acute MI was induced in 16 rabbits. Ten animals underwent cross-registered cine and contrast-enhanced CMR and histopathology at day 3 for assessment of MAR and IS (group#1). The remaining 6 rabbits had serial CMR for the study of LV remodelling (group#2).

**Results:** In group#1, mean IS was  $12.7 \pm 6.4\%$  and  $12.7 \pm 6.9\%$  of total LV myocardial mass on CMR (late-enhancement technique) and histopathology ( $P=0.52$ ;  $r=0.93$ ). No significant difference occurred between CMR and histopathology for the calculation of MAR and IS/MAR ratio ( $P=0.18$  and  $P=0.17$ ), whereas correlations were strong ( $r=0.92$  and  $r=0.95$ ).

In group#2, mean LV end-diastolic, end-systolic volumes and LV mass were significantly increased at 3 weeks compared with measurements at day 3 ( $P<0.01$ ). Significant correlations between initial IS and the increase in LV end-diastolic volume ( $r=0.66$ ) and the increase in LV mass ( $r=0.48$ ) were observed, as well as correlations between initial MAR and the increase in LV end-diastolic volume ( $r=0.70$ ) and the increase in LV mass ( $r=0.37$ ).

**Conclusions:** Comprehensive CMR provides accurate assessment of IS and MAR in reperfused rabbit MI. Infarct size is closely related to LV remodelling. Through the infarct size/MAR ratio, this approach has great potential for assessing interventions aimed at cardioprotection.

**Keywords.** Cardiac, magnetic resonance imaging, experimental study, myocardial infarction, left ventricular remodelling.

## **Introduction**

After the onset of a myocardial ischaemic insult, the determination of myocardial viability is of importance for the establishment of prognosis and for therapeutic purposes [1,2]. Contrast-enhanced cardiovascular magnetic resonance (CE-CMR) has emerged as a non-invasive imaging technique for myocardial infarction (MI) and tissue viability and for predicting the probability of recovery of left ventricular (LV) function [3-9]. However, the direct validation of CE-CMR for infarct sizing is not available in humans and the relation of the ischemic insult to LV myocardial remodeling is not fully understood. Measurement of infarct size (IS) by CMR is accurate in large animals [10-12], but these studies are restricted by ethical considerations, whereas in small animals, elevated heart rates and the small size of the heart make CMR challenging. IS by CE-CMR has been feasible in a rabbit model of acute non-reperfused MI, which is not the most common clinical presentation [13]. Furthermore, the myocardial area at risk (MAR) was not evaluated, whereas the distinction between MI and MAR is of importance for preclinical evaluation of therapeutic procedures tailored for cardioprotection [14]. The aims of the study were 1) to validate CMR for the assessment of MAR and IS in a rabbit model of reperfused MI, and 2) to study post-infarct LV remodelling and analyse the relation between ischaemic substrates and subsequent LV remodelling.

## **Materials and Methods**

### **Experimental study design**

All animal experiments were performed in an accredited lab in accordance with the official regulations provided by the French Ministry of Agriculture and with local ethical guidelines. Experiments were approved by the institutional animal care and use committee. We prospectively investigated two groups of rabbits. Group#1 included 10 rabbits with experimentally-induced reperfused acute MI that were studied for assessment of MAR and IS (CMR at day 3 following MI versus histopathology). Group#2 included 6 rabbits with the same experimental protocol of reperfused acute MI that were serially followed at day 3 (CMR#1) and 3 weeks (CMR#2), allowing for the study of post-infarct LV remodelling. Animals were then sacrificed at 3 weeks, immediately after CMR#2.

### **Experimental model of reperfused acute myocardial infarction**

Sixteen male New Zealand rabbits (2–2.5 kg) were anaesthetised, intubated and mechanically ventilated [15,16]. Under deep anaesthesia, a left thoracotomy was performed at the fourth intercostal space and a suture was passed beneath a major branch of the left coronary artery. Acute regional myocardial ischaemia was induced. In all animals, a coronary artery occlusion was performed lasting 30 to 45 minutes, followed by reflow. The chest was then closed in layers. All rabbits underwent CMR 72 h after coronary reflow.

### **Measurement of risk area and infarct size by histopathology**

The 10 rabbits of group#1 were sacrificed at day 3 immediately after CMR, whereas the 6 rabbits of group#2 were sacrificed after CMR#2 at 3 weeks. The ascending aorta was cannulated and perfused (120 mmHg) retrogradely with saline solution followed by Evans blue (5%) after ligation of the previously occluded artery to delineate MAR [16]. The LV

was cut into 6 contiguous 3 mm thick short-axis slices that were matched to CMR locations. These slices were weighed and incubated with 1% triphenyltetrazolium chloride (TTC, Sigma Chemical, Poole, Dorset, UK). Slices were fixed in 10% formaldehyde and then photographed with a digital camera. Using dedicated software (Scion Image, Scion Corporation, Frederick, MD), MAR and IS were determined by planimetry on digital frames: MAR and IS were identified as the non-blue region and as the TTC-unstained zone, respectively (Fig. 1). IS was measured as the TTC unstained region by planimetry on digital photographs taken from the series of 6 LV short axis slices. TTC unstained zones were manually planimeted, as was the whole LV myocardium. Similarly, the MAR was planimeted as the non-blue region on the series of short-axis views of the LV. The MAR was expressed as a percentage of LV weight and IS was expressed as a percentage of LV mass and of area at risk.

### **Cardiac magnetic resonance protocol**

Cardiac magnetic resonance (1.5 T Siemens Symphony<sup>®</sup>, Erlangen, Germany) was performed in anaesthetised animals (initiated by zolazepam and 20–30 mg/kg IV bolus pentobarbital sodium, and maintained with 2% isoflurane) in the right laterocubital position with electrocardiographic gating and short breath-hold acquisitions (the respirator was switched off). Heart rate was slowed down below 200 beats/min using a combination of inhaled 2% isoflurane and a 5 mg IV bolus of ivabradine (Servier, Courbevoie, France) if necessary. A flexible cardiac phased-array coil was wrapped around the chest for signal acquisition. Six contiguous short-axis locations encompassing LV from base to apex were acquired in the cine steady state free precession (SSFP) sequence (Fig. 1). The first location

at the base was prescribed 3 mm in front of the mitral ring at end-diastole. Typical imaging parameters of cine-CMR were optimised for cardiac imaging in rabbits (170 mm field of view, 256x160 image matrix, 0.7x1.0 mm<sup>2</sup> spatial resolution, 3 mm slice thickness, 2.6 ms repetition time, 1.6 ms echo time, imaging flip angle  $\alpha = 45^\circ$ , 20 ms temporal resolution, typically 35 s breath-hold time). For infarct imaging, cross-registered inversion-recovery 2D fast gradient-echo images were acquired at end-diastole 10 minutes after 2 ml IV bolus Gadolinium-DOTA injection (Dotarem<sup>®</sup>, Guerbet, Aulnay, France) (170 mm field of view, 256x160 image matrix, 0.7x1.0 mm<sup>2</sup> spatial resolution, 3 mm slice thickness, 3.1 ms repetition time, 1.6 ms echo time, imaging flip angle  $\alpha = 20^\circ$ , 220 ms typical inversion time (200-240 ms) (Fig. 1). For this sequence, the optimal inversion time was selected from a look-locker sequence to null the signal of non-infarcted myocardium

Short-axis cine-MR images were analysed for the assessment of LV volumes and mass (Argus<sup>®</sup> software, Siemens, Erlangen, Germany). The dysfunctional myocardium was assessed visually from the 6 short-axis locations as the planimetry of the surface of severely hypokinetic and/or akinetic myocardium, and then expressed as a percentage of the total LV mass for the estimation of MAR. Delayed-enhanced myocardium was planimeted on the series of cross-registered inversion-recovery short-axis images for precise delineation of myocardial infarction (Fig. 1). IS was measured by CMR using the late-enhancement technique 10 minutes after gadolinium injection. Delayed-enhanced myocardium was planimeted on the series of cross-registered inversion-recovery short-axis images for precise delineation of myocardial infarction. Infarct size was expressed as the percentage of total myocardial mass and as a percentage of MAR. CMR was compared with cross-registered histopathology with the same number of short-axis locations and same slice



thickness. When available, specific anatomical landmarks were used to check for correct cross-registration (distance from mitral ring, papillary muscles, RV-LV attachment points). CMR and histopathology were assessed by two independent observers.

### **Statistical analysis**

Continuous variables are presented as mean  $\pm$  SD and ranges, unless otherwise specified. Categorical data are presented as absolute values and percentages. Continuous and categorical variables were compared with use of the Chi-squared test, paired t tests, unpaired t tests or Fisher's exact test, as appropriate. Linear regression analysis was used to compare CMR and histopathology for the assessment of the MAR and IS, and for reproducibility measurements. Agreements between CMR and histopathology were evaluated using Bland-Altman plots. We analysed the data using the Stata<sup>®</sup> statistical software package, version 8.0 (Stata Corp, College Station, TX). All tests were two-tailed and a *P* value  $< 0.05$  was considered statistically significant.

### **Results**

CMR was interpretable in all rabbits and there was no mortality during the study period. Mean heart rate during CMR was  $178 \pm 11$  beats/min (range, 165-200). On histopathology, mean LV weight was  $4.7 \pm 0.8$  g in group#1 at day 3 and  $6.0 \pm 0.8$  g in group#2, 3 weeks after MI.

### **Infarct size and myocardial area at risk by CMR**

In group#1, there was no significant difference between CMR and histopathology for the assessment of IS. Mean IS expressed as the percentage of LV mass was  $12.7 \pm 6.4\%$  and  $12.7 \pm 6.9\%$  for CMR and histopathology (range 1-24%), respectively ( $P = 0.52$ ), with strong correlations between the 2 series of measurements (Fig. 2A). Mean MAR represented  $29.9 \pm 10.9\%$  and  $32.5 \pm 13.7\%$  of the total LV mass for CMR and histopathology, respectively ( $P = 0.18$ ) and the 2 series were highly correlated (Fig 2B). IS expressed as the percentage of MAR was  $40.8 \pm 19.2\%$  and  $36.7 \pm 16.1\%$  for CMR and histopathology, respectively ( $P = 0.17$ ), with strong correlations (Fig. 2C). The limits of agreement for IS, expressed as a percentage of LV mass and as a percentage of the MAR, were good between CMR and histopathology, with 95% confidence intervals of -3.8 to +4.8% and -9.4 to +10.7%, respectively. The limits of agreement for the MAR were in the range of -13.3 to +7.9% with a 95% confidence interval (Fig 2).

In group#1, intra- and interobserver reproducibility for CMR measurements of IS ( $y = 0.99x - 0.09$ ,  $r = 0.98$ , standardised error (SE) = 0.06; and  $y = 0.95x + 0.58$ ,  $r = 0.94$ , SE = 0.13, respectively, all  $P < 0.001$ ) and MAR ( $y = 1.03x - 0.41$ ,  $r = 0.97$ , SE = 0.10; and  $y = 1.05x + 0.17$ ,  $r = 0.93$ , SE = 0.14, respectively, all  $P < 0.001$ ) were good.

### **Post-infarct left ventricular remodelling**

In group#2, there were good agreement and correlations for the determination of IS between CMR and histopathology ( $10 \pm 3\%$  versus  $9 \pm 3\%$  of total LV mass,  $P = 0.17$ ;  $r = 0.85$ ,  $P < 0.0001$ ). Mean LV end-diastolic and end-systolic volumes and mean LV mass were significantly increased at 3 weeks compared with measurements at day 3 (Table 1).

In these animals, IS expressed as total infarct mass, slightly increased over time between day 3 and 3 weeks ( $0.6 \pm 0.1$  g versus  $0.7 \pm 0.2$  g,  $P = 0.05$ ). When expressed as percentage of the LV mass, IS decreased significantly over time ( $15.2 \pm 5.0\%$  versus  $11.8 \pm 3.1\%$ ,  $P = 0.02$ ). Significant correlations were observed between initial IS by CMR at day 3 and the increase in LV end-diastolic volume ( $r = 0.66$ ,  $P < 0.001$ ), and between initial IS by CMR and the increase in LV mass ( $r = 0.48$ ,  $P < 0.001$ ). Although less pronounced, this relation was also observed between initial IS on CE-CMR and the subsequent increase in LV end-systolic volume ( $r = 0.27$ ,  $P < 0.05$ ). Interestingly, correlations were also observed between initial MAR by CMR at day 3 and the increase in LV end-diastolic volume ( $r = 0.70$ ,  $P < 0.01$ ), and between initial MAR by CMR at day 3 and the increase in LV mass ( $r = 0.37$ ,  $P < 0.05$ ).

## Discussion

The main results of the present study are: 1) comprehensive CMR provides accurate assessment of IS and MAR in a rabbit model of reperfused myocardial infarction; 2) the determination of IS is accurate at the 3-week follow-up with the extravascular contrast agent used; 3) this animal model seems promising for the longitudinal study of LV remodelling; 4) the accurate assessment of the IS/MAR ratio could allow the longitudinal evaluation of targeted strategies aimed at cardioprotection.

Barkhausen et al. [13] have demonstrated the accuracy of the standard Gadolinium-based extracellular contrast agent to assess IS in a rabbit model of non-reperfused acute MI. The present report offers the advantage of studying myocardial distribution of Gd-DOTA at the acute phase and at the 3-week follow-up in an experimental model of brief coronary artery occlusion followed by reflow, which is the most common clinical presentation. The time for coronary occlusion has been selected on the basis of previous experimental studies which provided a wide range of infarct size and a clear delineation between myocardial infarct and the area at risk (15,16). Compared with histopathology, there was no overestimation of IS in the present model. It is likely that differences between histopathology and CE-CMR in IS can, at least in part, be explained by partial volume effects [12]. In the current report, partial volume effect might be significantly decreased because of the use of thin slices [13]. Also, hyperenhancement in the peri-infarction zone seen with Gadolinium chelates has been mainly reported within the first 24h following induction of acute MI [17]. In our study, the first CMR was performed 3 days after induction of MI, which may concur to explain the lack of IS overestimation, and which

mimics the usual clinical scenario after the onset of acute coronary syndrome. In addition, comprehensive cross-registered evaluation of dyskinetic myocardium on cine-CMR was used to assess MAR. In comparison with the Evans Blue staining, the current study shows that the size of the MAR can be determined using this visual approach, although the lack of direct imaging of the myocardial area at risk was a clear limitation. Thus, the infarct size/MAR ratio can be assessed with this comprehensive approach. In the experimental setting, this ratio represents the crucial quantitative index for the evaluation of novel therapies aimed at cardioprotection such as pharmacological approaches, cell therapy or post-conditioning techniques [15].

During coronary occlusion, the visual control of the epicardial surface along with the prompt release of the snare for coronary reflow enabled a wide range of IS to be obtained, i.e. from 1 to 24% of the LV mass. In addition, the robustness of the model allows for a 3-week follow-up of the animals after induction of MI, which enabled the study of post-infarct LV remodelling. Therefore, the present experimental study permits a non-invasive analysis of the relationship between the size of the initial ischaemic damage and subsequent LV remodelling, showing good correlations between the size of induced MI and the subsequent increase in LV mass and volumes. As suggested by others [18], the current data support the concept that the presence and extent of dysfunctional viable myocardium may represent a determinant of subsequent LV remodelling. In vivo serial CMR imaging was restricted in larger animals such as dogs or pigs [3,10-12,19,20]. Among the various advantages of the current rabbit model, one can point out the possibility of studying several animals in one imaging session, with easier applicability and at lower costs. The possibility of serial non-invasive imaging is crucial for the analysis of LV remodelling but also for

longitudinal assessment in the same animals of targeted interventions designed to impact on the infarct size/MAR ratio.

Because of elevated heart rates and short diastolic times, T2-weighted black blood spin echo CMR imaging could not be performed and represents a limitation. It is known that the T2-enhanced area corresponds to the location of ischaemic injury but overestimates IS [19,20]. T2 changes are indicative of the presence of oedema rather than the area of damaged myocardium itself [21-23]. More importantly, these non-contrast-enhanced imaging techniques have limited signal-to-noise and contrast-to-noise ratios and most authors found it difficult to precisely distinguish infarcted from non-infarcted myocardium. Increased T2 signal has low specificity for the detection of myocardial necrosis, and T2 alterations are less consistent especially for the detection of chronic myocardial infarction [21]. The current experiments were performed on a 1.5T MR clinical system. To our knowledge, there are no available data on segmented T2-weighted imaging after induced infarction at higher magnetic fields in rabbits. Finally, the delineation between myocardial infarction and the area at risk is clearly dependent on the amount of collaterals, which is highly variable in different animal species and in humans.

## **Conclusion**

Comprehensive CMR provides accurate assessment of IS and MAR in a rabbit model. The determination of IS is accurate at the 3-week-follow up with the extravascular contrast agent used. Serial imaging demonstrated a close relationship between initial IS, the extent of initially dysfunctional myocardium, and subsequent LV remodelling. Through the accurate assessment of the infarct size/MAR ratio and the use of serial non-invasive

imaging, this approach has accurate potential for the longitudinal evaluation of targeted interventions aimed at cardioprotection.

## References

1. Allman KC, Shaw LJ, Hachamovitch R et al (2002) Myocardial viability testing and impact of revascularisation on prognosis in patients with coronary artery disease and left ventricular dysfunction : a meta-analysis. *J Am Coll Cardiol* 39:1151–1158.
2. Bax JJ, Poldermans D, Elhendy A, et al (1999) Improvement o left ventricular ejection fraction, heart failure symptoms and prognosis after revascularization in patients with chronic coronary artery disease and viable myocardium detected by dobutamine stress echocardiography. *J Am Coll Cardiol* 34:163-169.
3. Kim RJ, Wu E, Rafael A, et al (2000) The use of contrast-enhanced MRI to identify reversible myocardial dysfunction. *N Engl J Med* 343:1445-1453.
4. Nijveldt R, Hofman MBM, Hirsch A, et al. Assessment of microvascular obstruction and prediction of short-term remodeling after acute myocardial infarction: cardiac MR imaging study. *Radiology* 2009;250:363-370.
5. Gerber BL, Garot J, Bluemke DA, et al. Accuracy of contrast-enhanced magnetic resonance imaging in predicting improvement of regional myocardial function in patients after acute myocardial infarction. *Circulation* 2002;106:1083-1089.
6. Kuhl HP, Beek AM, van der Weerd AP, et al (2003) Myocardial viability in chronic ischemic heart disease: comparison of contrast-enhanced magnetic resonance imaging with (18)F-fluorodeoxyglucose positron emission tomography. *J Am Coll Cardiol* 41:1341-1348.



7. Wagner A, Mahrholdt H, Holly TA, et al. Contrast-enhanced MRI and routine single photon emission computed tomography (SPECT) perfusion imaging for detection of subendocardial myocardial infarcts: an imaging study. *Lancet* 2003;361:374-379.
8. Cochet AA, Lorgis L, Lalande A, Zeller M, Beer JC, Walker PM, Touzery C, Wolf JE, Brunotte F, Cottin Y (2009) Major prognostic impact of persistent microvascular obstruction as assessed by contrast-enhanced cardiac magnetic resonance in reperfused acute myocardial infarction. *Eur Radiol* 19:2117–2126.
9. Hunold P, Schlosser T, Barkhausen J (2006) Magnetic resonance cardiac perfusion imaging - a clinical perspective. *Eur Radiol* 16:1779-1188.
10. Kim RJ, Chen EL, Lima JA, et al. Myocardial Gd-DTPA kinetics determine MRI contrast enhancement and reflect the extent and severity of myocardial injury after acute reperfused infarction. *Circulation* 1996;94:3318-3326.
11. Kim RJ, Fieno DS, Parrish TB, et al. Relationship of MRI delayed contrast enhancement to irreversible injury, infarct age, and contractile function. *Circulation* 1999;100:1992-2002.
12. Fieno DS, Kim RJ, Chen EL, et al (2000) Contrast-enhanced magnetic resonance imaging of myocardium at risk: distinction between reversible and irreversible injury throughout infarct healing. *J Am Coll Cardio* 136:1985-1991.
13. Barkhausen J, Ebert W, Debatin JF, et al (2002) Imaging of myocardial infarction: comparison of Magnevist and Gadophrin-3 in rabbits. *J Am Coll Cardiol* 39:1392-1398.
14. Yellon DM, Baxter GF. Protecting the ischaemic and reperfused myocardium in acute myocardial infarction: distant dream or near reality? *Heart* 2000;83:381-387.

15. Tissier R, Aouam K, Berdeaux A, Ghaleh B. Evidence for a ceiling of cardioprotection with a nitric oxide donor-induced delayed preconditioning in rabbits. *J Pharmacol Exp Ther* 2003;306:528–531.
16. Tissier R, Waintraub X, Couvreur N, et al. Pharmacological postconditioning with the phytoestrogen genistein. *J Mol Cell Cardiol* 2007;42:79-87.
17. Saeed M, Bremerich J, Wendland MF, et al. Reperfused myocardial infarction as seen with use of necrosis-specific versus standard extracellular contrast agents in rats. *Radiology* 1999;213:247-257.
18. Carluccio E, Biagioli P, Alunni G, et al (2006) Patients with hibernating myocardium show altered left ventricular volumes and shape, which revert after revascularization: evidence that dyssynergy might directly induce cardiac remodeling. *J Am Coll Cardiol* 47:969-977.
19. Pflugfelder PW, Wisenberg G, Prato FS, et al (1986) Serial imaging of canine myocardial infarction by in vivo nuclear magnetic resonance. *J Am Coll Cardiol* 7:843-849.
20. Caputo GR, Sechtem U, Tscholakoff D, et al. Measurements of myocardial infarct size at early and late time intervals using MR imaging: an experimental study in dogs. *Am J Roentgenol* 1987;149:237-242.
21. Johnston DL, Homma S, Liu P, et al. Serial changes in nuclear magnetic resonance relaxation times after myocardial infarction in the rabbit: relationship to water content, severity of ischemia, and histopathology over a six-month period. *Magn Reson Med* 1988;8:363-379.

22. Ryan T, Tarver RD, Duerk JL, et al (1990) Distinguishing viable from infarcted myocardium after experimental ischemia and reperfusion by using nuclear magnetic resonance imaging. *J Am Coll Cardiol* 15:1355-1364.
23. Bouchard A, Reeves RC, Cranney G, et al. Assessment of myocardial infarct size by means of T2-weighted 1H nuclear magnetic resonance imaging. *Am Heart J* 1989;117:281-289.

## Figure Legends

**Figure 1. A.** Still frames extracted from the steady-state free precession cine-CMR at the mid LV level during end-diastole (upper left) and end-systole (upper right), along with matched delayed CE-CMR (bottom left) and corresponding histopathology (bottom right) in an animal for which experimental coronary occlusion led to a small MAR (16% of total LV mass, 30% of LV mass in this short-axis location) and limited MI (6% of total LV mass, 14% of LV mass in this short-axis location). The MAR was assessed by the extent of severely dyskinetic myocardium on cine CMR (arrows) and the Evans blue unstained tissue on histopathology, whereas infarction appeared as the enhanced region on delayed contrast CMR (arrows) and unstained (non-red) region on TTC stain (arrows). **B.** CMR data acquired at the LV apical level in another animal with an extensive MAR (38% of total LV mass, 82% of LV mass in this slice location, arrows) and large infarct (17% of total LV mass, 76% of LV mass in this slice location) on CE-CMR (arrows) and corresponding TTC stain (arrows). **C.** CMR data acquired at the LV apical level in another animal with mild MAR (24% of total LV mass, 48% of LV mass in this short-axis location) and mild MI (11% of total LV mass, 20% of LV mass in this short-axis location). LV: left ventricular, MAR: myocardial area at risk, MI: myocardial infarction, CE-CMR: contrast-enhanced cardiac magnetic resonance.

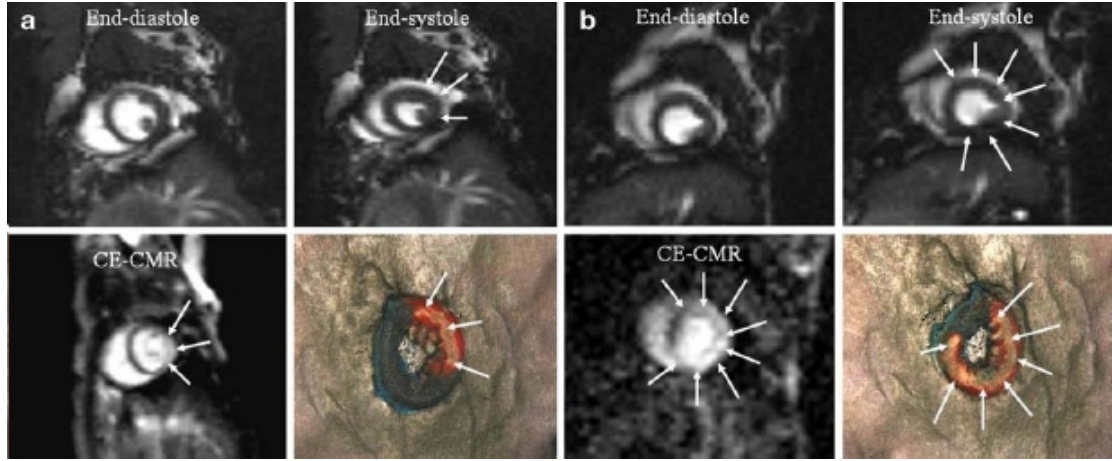
**Figure 2.** Linear regression (*left*) and Bland-Altman plots (*right*) for comparisons of infarct size (IS) (upper panel **[A]**), myocardial area at risk (MAR) (mid panel **[B]**), and IS/MAR ratio (lower panel **[C]**) as assessed by CMR and histopathology.

**Table 1.** Left ventricular alterations after reperfused myocardial infarction assessed by CMR in group#2

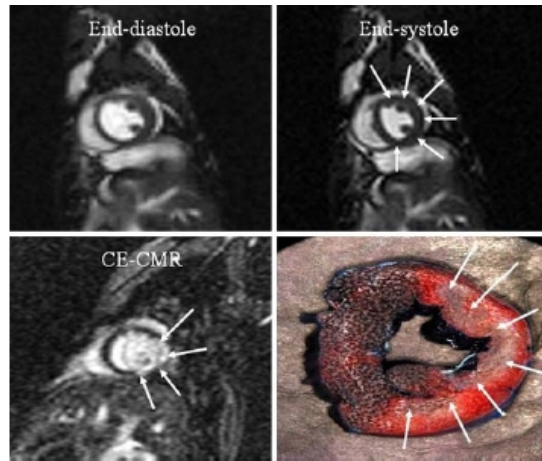
	CMR#1	CMR#2	P Value
Left ventricular end-diastolic volume (ml)	3.7 ± 0.5	4.7 ± 0.4	0.0006
Left ventricular end-systolic volume (ml)	2.7 ± 0.6	3.4 ± 0.4	0.01
Left ventricular mass (g)	4.72 ± 0.55	5.22 ± 0.46	0.01

CMR#1 = cardiac magnetic resonance at day 3; CMR#2 = CMR 3 weeks later

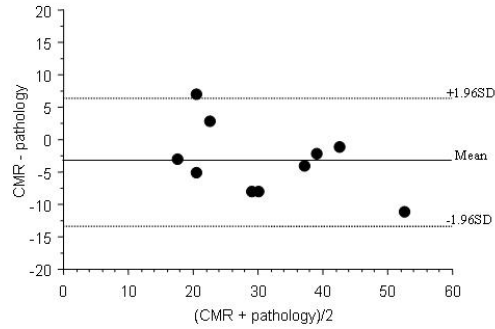
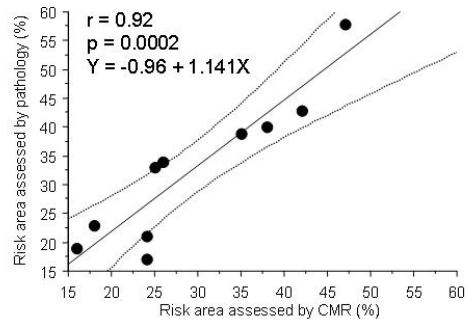
**A**



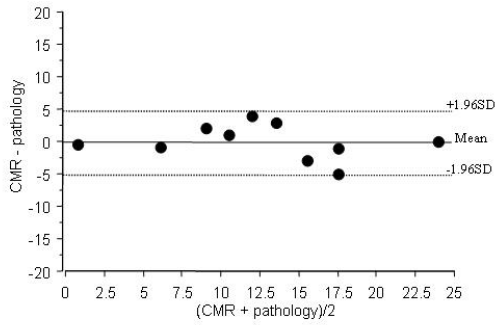
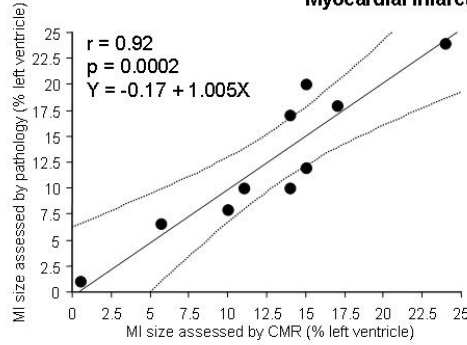
**B**



**Area of risk (% of left ventricle)**



**Myocardial infarct size (% of left ventricle)**



**Myocardial infarct size (% area of risk)**

